Marco J. da Silva
mdasilva@utfpr.edu.br
Universidade Tecnológica Federal do Paraná
Department of Electrical Engineering (CPGEI)
80230-901 Curitiba, Paraná, Brazil

Uwe Hampel
u.hampel@hzdr.de
Helmholtz-Zentrum Dresden-Rossendorf e.V.
Institute of Safety Research
01328 Dresden, Saxony, Germany

Lúcia V. R. Arruda
lvrarruda@utfpr.edu.br
Universidade Tecnológica Federal do Paraná
Department of Electrical Engineering (CPGEI)
80230-901 Curitiba, Paraná, Brazil

Carlos E. F. do Amaral
camaral@utfpr.edu.br
Universidade Tecnológica Federal do Paraná
Department of Electrical Engineering (CPGEI)
80230-901 Curitiba, Paraná, Brazil

Rigoberto E. M. Morales
rmorales@utfpr.edu.br
Universidade Tecnológica Federal do Paraná
Department of Mechanical Engineering (PPGEM)
80230-901 Curitiba, Paraná, Brazil

Experimental Investigation of Horizontal Gas-Liquid Slug Flow by Means of Wire-Mesh Sensor

The monitoring and visualization of two-phase flow is of great importance either from technical/practical point of view for process control and supervision or from scientific/theoretical point of view, for the understanding of physical phenomenon. A wire-mesh sensor was applied to experimentally investigate two-phase horizontal pipe flow. Furthermore, some physical flow parameters were extracted based on the raw measured data obtained by the sensor. In this article, first, the work principle of wire-mesh sensors is revised and, second, the methodology of flow parameter extraction is described. A horizontal flow test section comprising of a pipe of 26 mm i.d. 9 m long was employed to generate slug flows under controlled conditions. An 8 × 8 wire-mesh sensor installed at the end of the test section delivers cross-sectional images of void fraction. Based on the raw data, mean void fraction, time series of void fraction and characteristic slug frequency are extracted and analyzed for several experiments with different liquid and gas superficial velocities.
Keywords: *two-phase flow, slug flow, wire-mesh sensor, void fraction, time series, flow visualization*

Introduction

Gas-liquid two-phase flows are present in many industrial applications, such as chemical, oil and nuclear industries. In many cases, such flows determine the operation efficiency and security of the equipment and process where they occur. In this way, experimental investigations of two-phase flows are very important not only for a better understanding of the phenomena involved, but also to offer a trustful experimental data base in order to help, for example, the development of theoretical models or the validation of predictions from computer simulations such as performed by Computational Fluid Dynamics (CFD) software. In addition, advanced measurement techniques are also necessary in industrial applications in order to allow for the monitoring and control of processes.

Many experimental techniques have been used to analyze two-phase flows so far, among them conductive and capacitive probes (Ahmed and Ismail, 2008), high-speed videometry (Guevara-López et al., 2008), and more complex techniques such as x-ray and gamma ray tomography (Hervieu, Jouet and Desbat, 2002). However, none of the proposed techniques can claim a universal applicability and some of them have considerable drawbacks and may fail in particular practical situations.

Wire-mesh sensors are flow imaging devices and allow the investigation of multiphase flows with high spatial and temporal resolution (Prasser, Bottger and Zschau, 1998) and overcame many of the drawbacks of alternative techniques. The sensor is a hybrid solution in between intrusive local measurement of phase fraction and tomographic cross-sectional imaging (for details see next section). This type of sensor has been successfully employed by a number of researchers to investigate two-phase flow in the past. The first generation of wire-mesh sensors is based on conductivity measurements. Recently, the capacitance wire-mesh sensor has been developed and tested, which allow the investigation of non-conducting fluids too, such as oil or organic liquids (Da Silva, Schleicher and Hampel, 2007).

The intrusiveness effect of wire-mesh sensors has been extensively investigated in the past, for instance wire-mesh measurements were evaluated against high-speed filming (Wangjiraniran et al., 2003), a fast x-ray tomography system (Prasser, Misawa and Tiseanu, 2005) and gamma-ray densitometry (Sharaf et al., 2010). In short, the results have shown that the sensor yields images of an undisturbed flow, and regarding void fraction measurement, uncertainty was found to be in the 10% range. Thus, wire-mesh sensors seem to be an excellent tool to experimentally investigate two-phase gas-liquid slug flows.

In this experimental study, the wire-mesh technique based on capacitance measurements is applied to study two-phase slug flows in horizontal pipes. Based in raw data measured it is possible to extract some specific parameters of interest. The wire-mesh technique allows investigating the flow nature with good degree of details due its good spatial and temporal resolution. Based in the raw data, it is possible to extract some specific parameters of interest such as mean void fraction, cross-section averaged void fraction and characteristic slug frequency. Firstly, this paper reviews the work principle of the wire-mesh technique, following, it details the methodology to extract parameters of interest of two-phase liquid-gas slug flow.

Nomenclature

a = *coefficients, dimensionless*
C_0 = *constant, dimensionless*
D = *pipe diameter, m*
g = *gravitational constant, 9.81 m/s*^{2}

i = *spatial index (rows), dimensionless*
j = *spatial index (columns), dimensionles*
k = *time index, dimensionless*
N = *total number of time samples, dimensionless*
J_L = *liquid superficial velocity, m/s*
J_G = *gas superficial velocity, m/s*
J = *two-phase mixture superficial velocity, m/s*
f = *frequency, Hz*
v_{gd} = *drift velocity, m/s*
V = *electrical voltage, V*

Greek Symbols

α = *void fraction, dimensionless*
$\overline{\alpha}$ = *mean void fraction, dimensionless*

Subscripts

L = *low*
H = *high*

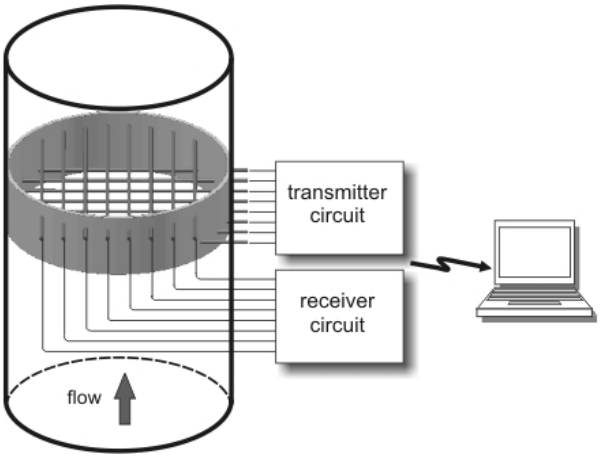

Figure 1. Schematic representation of a wire-mesh sensor.

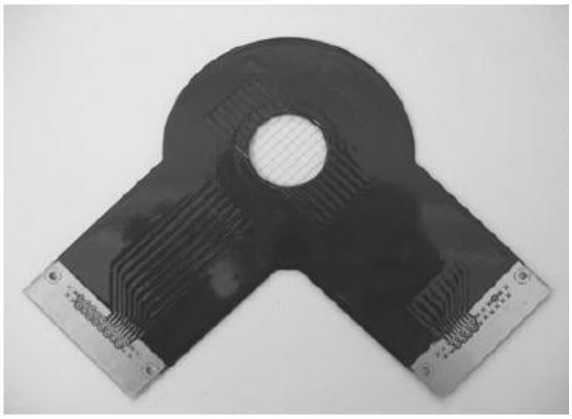

Figure 2. Photography of a 8 × 8 electrode sensor used in this measurement.

Wire-Mesh Sensor

The wire-mesh sensor comprises of two sets of wires (electrodes) stretched over the cross-section of a vessel or pipe forming a grid of electrodes, as schematically depicted in Fig. 1 (Prasser, Bottger and Zschau, 1998; Da Silva, Schleicher and Hampel, 2007). Each plane of parallel wires is positioned perpendicular to each other with a small axial separation between them of 1.5 mm. In each layer there are eight stainless steel wires with diameter of 100 μm spaced 3.25 mm between them. Figure 2 shows a picture of the sensor used in this study. The associated electronics applies a 5 MHz sinus signal to measure the local capacitance in the gaps of all crossing points at high repetition rate through a multiplexed approach. Each of the measured signals reflects the constitution of the flow within its associated sub-region, i.e. each crossing point acts as local phase indicator. Hence, the set of data obtained from the sensor directly represents the phase distribution over the cross-section and no reconstruction procedure is needed as usual for tomographic imaging systems. A complete image is measured with up to 1 kHz frame rate. Therefore, this technique allows the visualization of the cross-sectional phase distributions with a high temporal resolution.

Data processing and analysis

The voltage levels measured by the wire-mesh sensor are stored in a three-dimensional matrix at the computer memory $V(i,j,k)$, with k being the time index and i and j spatial indexes respectively (Da Silva, Schleicher and Hampel, 2007). In fact, wire-mesh sensor electronics generate voltages with a logarithmic response, which is assumed to be previously known and adjusted to a linear response (for further details Da Silva et al., 2009). In this way, the measured voltages are proportional to the electrical permittivity ε of each crossing point, which in turn is proportional to the void fraction. In order to convert the measured voltages to permittivity values and further obtain the phase fraction distributions, a calibration routine is used. First, a measurement of a matrix V_L for a substance of low permittivity covering the whole sensor cross-section is performed. The procedure is then repeated with the entire cross-section covered with another substance having a higher permittivity V_H, which gives a second reference data matrix. In this way the void fraction α can be obtained by

$$\alpha(i,j,k) = \frac{V_H(i,j) - V(i,j,k)}{V_H(i,j) - V_L(i,j)} \tag{1}$$

To analyze the void fraction data $\alpha(i,j,k)$, which is a 3D matrix, different levels of complexity were used. Images sequences of the flow as well as cross section images from the pipeline can be generated. Important quantitative insights of the flow are obtained by averaging the measured void fraction in space and/or time. Hence, averaging the data over cross section, time series of the void fraction can be obtained in the form

$$\alpha(k) = \sum_i \sum_j a(i,j) \cdot \alpha(i,j,k), \tag{2}$$

where $a(i,j)$ is the contribution of each crossing point (i,j) for the total cross section area (details in Prasser, Krepper and Lucas, 2002). These time series $\alpha(k)$ can be analyzed by a histogram (Probability Density Functions – PDF) or by their spectral components. This last analysis is performed through the estimation of the power spectral density function (PSD), by the Welch modified periodogram (Marple, 1987). Through the PSD it is possible to identify the characteristic frequency of the bubbles and slugs in the studied flows.

In the last and lower level of complexity, the 3D data matrix is integrated in its three components resulting in the mean void fraction during the experiment, in the form of Eq. (3).

$$\overline{\alpha} = \frac{1}{N} \sum_{k=1}^{N} \alpha(k) \tag{3}$$

where N is the total number of time samples of the signal.

Experimental Test Facility

The experiments were performed in the Thermal Sciences Laboratory (LACIT) at Universidade Tecnológica Federal do Parana (UTFPR), in which an experimental flow loop is available to produce different flow patterns of air-water mixtures. The flow loop comprises a horizontal acrylic pipe of 26 mm diameter and 9.0 m long and associated devices to produce a two-phase flow under controlled conditions (Fig. 3). Tap water (electrical conductivity of 380 μs/cm) and air were used as fluids and their flow rates are independently measured by means of a Coriolis flow meter for water and a rotameter for air. Water is circulated in close loop with help of a pump. The air coming from a compressor is mixed with the flowing water in the pipe entrance through a gas-liquid mixer. In the pipe exit, there is a separator/reservatory, where air is expelled to the atmosphere and water is stored.

A wire-mesh sensor is installed 7.5 m from the pipe entrance, (288 times internal diameter). In this way, relatively well developed flow is expected to be evaluated. Water temperature as well as air temperature and pressure at pipe entrance are monitored by means of industrial sensors connected by a Foundation Field Bus and controlled by a host computer running a supervisory program. Furthermore, the absolute pressure of two-phase mixture close to the measurement plane, where the wire-mesh sensor is installed, is measured. This value is used to obtain the exact air flow rate at the measurement point, i.e. rotameter readings are compensated by the pressure difference at pipe entrance and pressure at measurement plane. Figure 3 shows the schematic of the test facility and Fig. 4 shows photography of the wire-mesh sensor installed in the experimental flow loop.

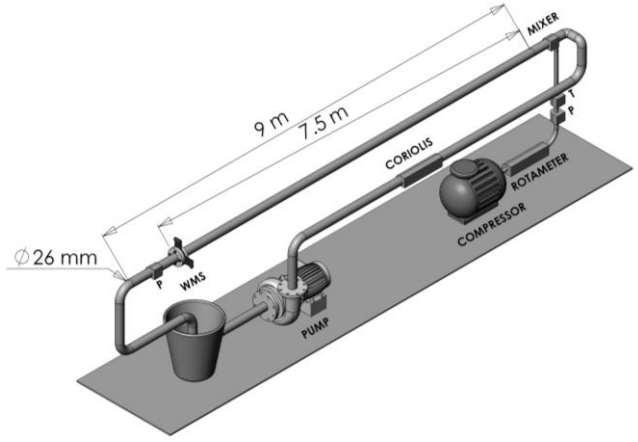

Figure 3. Schematic representation of the measurement plant. P and T denote respectively pressure and temperature transducers.

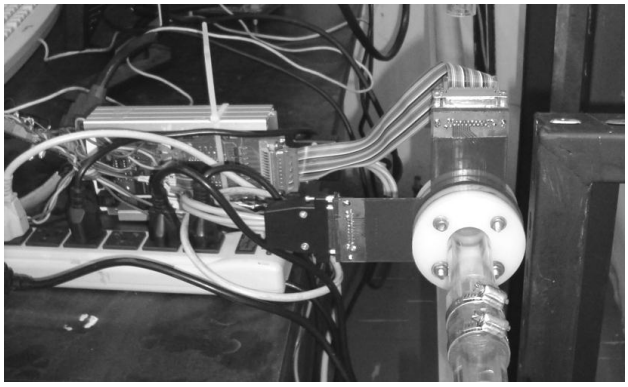

Figure 4. Photography of the wire-mesh sensor installed in the experimental flow test section.

Results

Twelve experiments were performed at different gas and liquid superficial velocities, as shown in Table 1. All experiments fall within the range of slug flow pattern. For each experiment, data from the wire-mesh sensor was measured for 240 seconds with a repetition rate of 500 Hz. Before the flow measurements were carried out, reference measurements of empty and full pipe were collected, i.e. matrices V_H e V_L, in order to measure the values of the void fraction by Eq. (1).

As described earlier, different degrees of complexity were used to analyze the measured signals/images. Figure 5 shows images obtained from wire-mesh sensor measurements for the experiment 1 (J_L = 0.3 m/s, J_G = 0.7 m/s). The liquid is shown in dark and the gas in light color. These images offer qualitative insight of the flow. Figure 5(a) shows a sequence of images with details of one single bubble. Here one can note the round shape of the bubble's nose and the flat shape of the bubble's tail. Figure 5(b) shows a lateral view of the flow, which was measured taking the data of the central electrode of the sensor, i.e. an axial chord through the pipe center.

Quantitative results can be obtained from the void fraction data. Hence, Table 1 shows the values of the mean void fraction $\bar{\alpha}$ calculated by Eq. (3) from the data measured for the total time of 240 seconds, which represents N = 120,000 at the measured frequency of 500 Hz. Figure 6 shows the relationship between $\bar{\alpha}$ and the quotient J_G/J, where J is the superficial velocity of the mixture = $J_G + J_L$. Experimental data were compared with correlations from the literature (Table 2), showing good agreement as depicted in Fig. 6. Furthermore, the correlation seems to have a linear behavior, as also recently observed by Szaliski et al. (2010) in the case of vertical slug flow.

Table 1. Experimental conditions adopted for liquid superficial velocities (J_L) and gas (J_G), as well as values of mean void fraction and characteristic frequency of the flow for 240 seconds.

Exp #	J_L (m/s)	J_G (m/s)	$\bar{\alpha}$ (%)	f (Hz)
1	0.3	0.5	28.61	0.49
2	0.3	0.7	42.15	0.73
3	0.3	1	51.46	0.61
4	0.3	1.3	54.69	0.61
5	0.3	1.5	58.41	0.49
6	0.3	2	61.49	0.61
7	0.5	0.3	22.47	1.46
8	0.5	0.5	32.58	1.46
9	0.5	0.7	41.04	0.98
10	0.7	0.7	37.98	2.20
11	0.7	1	47.24	1.83
12	0.7	1.3	52.33	1.71

Table 2. Correlations for prediction of void fraction α.

Reference	Correlation	Eq.
Gregory and Scott (1969)	$\bar{\alpha} = \frac{J_G}{1.19J}$	(4)
Mattar and Gregory (1974)	$\bar{\alpha} = \frac{J_G}{1.3J + 0.7}$	(5)

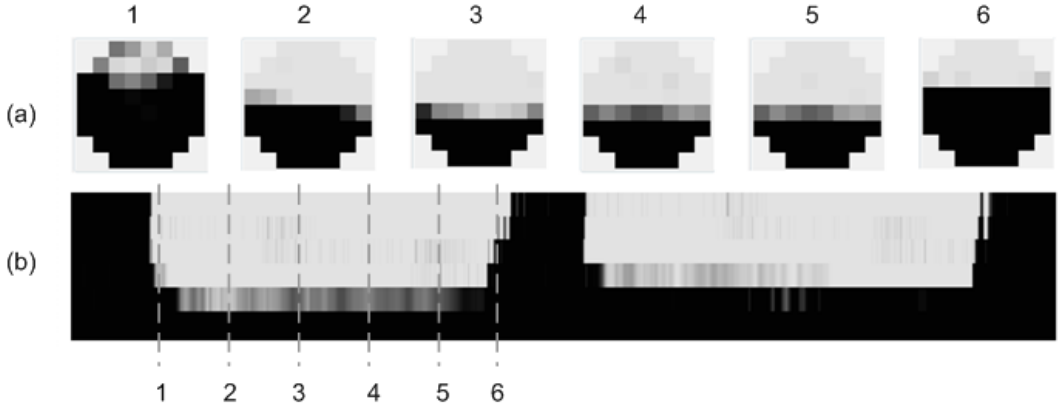

Figure 5. Images of experiment #1 (J_L = 0,3 m/s, J_G = 0,7 m/s). (a) Sequence of cross-section images showing details of a single bubble. (b) Lateral view of the flow (axial chord through the center of the pipe).

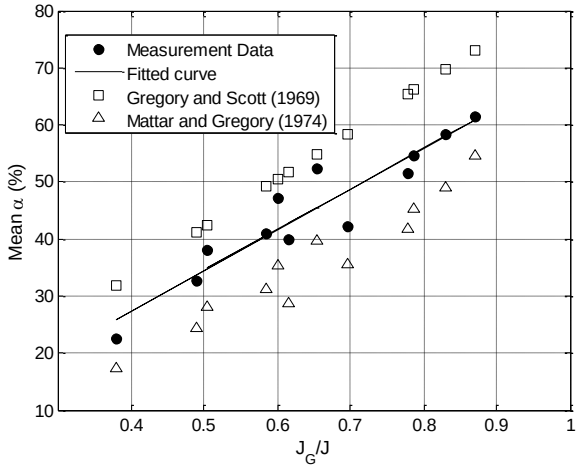

Figure 6. Void fraction versus the ratio J_G/J.

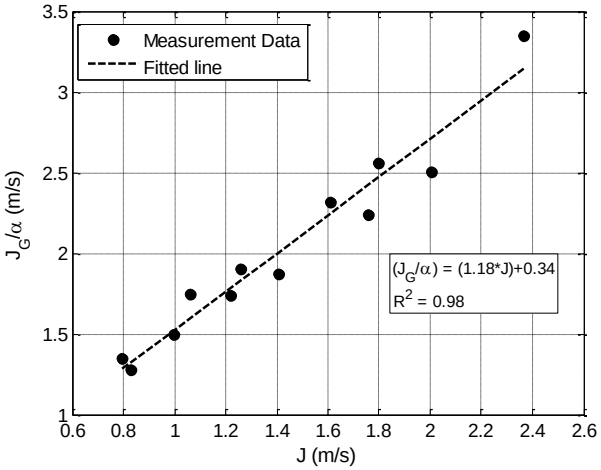

Figure 7. Measured gas velocity (J_G/α) against mixture velocity along with the best fit line to obtain the parameters of Eq. (6).

In order to further validate our experimental data, we analyze the present data with respect to the general formulation due to Zuber and Findlay (1965) which applied the drift flux model to develop a series of correlations for prediction of flow parameters such as the void fraction. They equated the in-situ gas velocity (J_G/α) as being a linear function in the form

$$\frac{J_G}{\alpha} = C_0 J + v_{gd} \,, \tag{6}$$

where C_0 is a constant and v_{gd} the drift velocity. Figure 7 depicts the experimental data and the best fit line. Hence, in the present work C_0 was found to be 1.18 and v_{gd} = 0.34, which are consistent with the values from Zuber and Findlay (1965), which suggested C_0 = 1.13 and v_{gd} = 0.23 (for air and water).

The void fraction time series $\alpha(k)$ obtained by Eq. (2) for all experiments are shown in Fig. 8. All the curves have a shape similar to a square wave with a plateau in $\alpha \approx 0$, characterizing the passage of a liquid slug and other plateau with an intermediary α, characterizing the flow of a bubble. Obviously, passing frequencies and amplitudes are different for each experimental condition used. The bimodal distribution of the time series values can be observed clearly in Fig. 9, where the histograms of this series are shown. One can see that the bubbles size increase proportionally with J_G and while keeping J_L constant (exp. 2 to 5), since the distribution curve moves to the right.

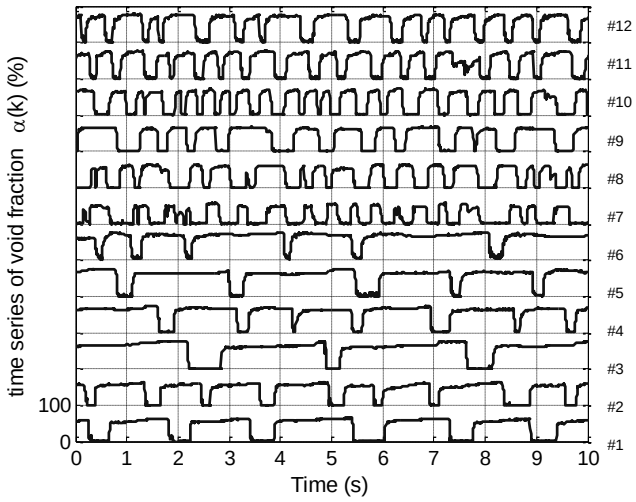

Figure 8. Time series of void fractions $\alpha(k)$ showing only 10 s of the 240 s measured.

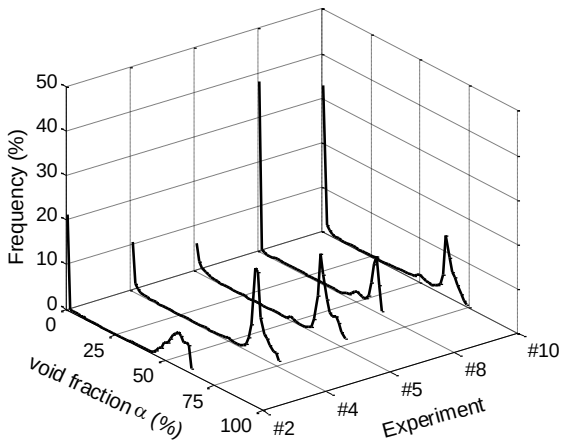

Figure 9. Histograms of the time series for selected experimental conditions.

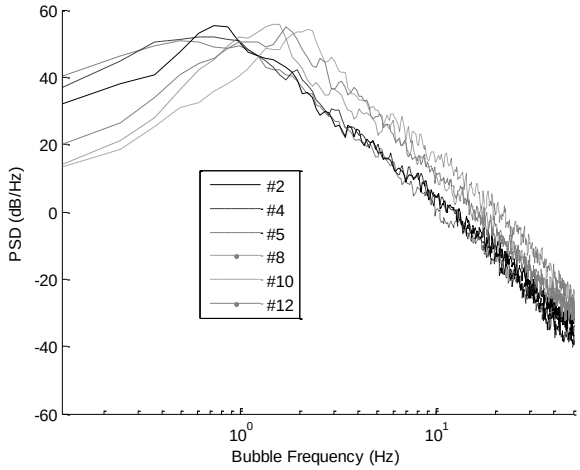

Figure 10. PSDs of the time series signals for selected experimental conditions.

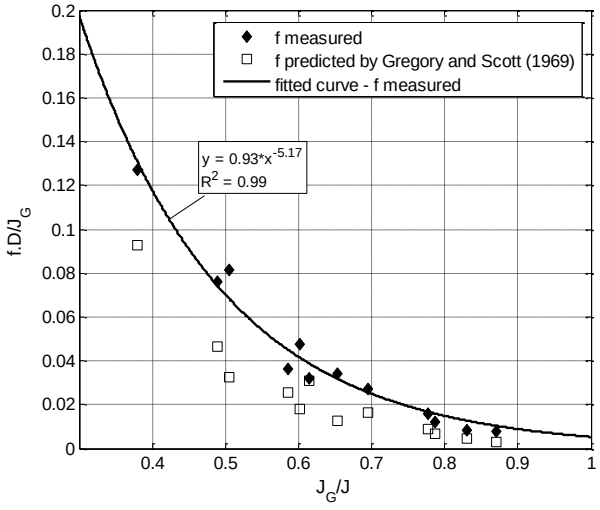

Figure 11. Variation of the frequency $f \cdot D/J_G$ versus J_G/J.

To analyze the characteristic frequency the calculation of PSD (section 2) was used. In Fig. 10 the spectra of the time series signals are shown. All the curves have a similar shape with a peak in the low frequencies, characterized by the typical alternating frequency of the slug flow. We defined the peak value of the PSD curves as the characteristic frequency of the slug unities. Hence, the frequencies obtained are shown in Table 1. Frequencies around the unity were found for all experiments. In Fig. 11, the variation of the normalized parameter $f \cdot D/J_G$ versus J_G/J is shown, where D is the pipe diameter. One can observe an exponential tendency typical of the slug flow. In addition to the experimental data, data based on correlation from Gregory and Scott (1969) is also presented, showing a good agreement:

$$f = 0,0266\left[\frac{J_L}{gD}\left(\frac{19.75}{J} + J\right)\right]^{1.2} \tag{7}$$

Conclusions

We have reviewed the operation principle of the wire-mesh sensor, as well as the methodology for extraction of some quantitative parameters of the flow based in the raw data measured. This methodology was applied to a series of experiments of horizontal slug flow, showing some details of the studied flow. Therefore, the wire-mesh technique is a powerful tool in the investigation of two-phase flows, since it can show with details the flow in different degrees of complexity. Based in these experimental data, more information about the behavior of the two-phase flow can be obtained as well as such experimental data can support the development of new theoretical models or the improvement of the existent models of two-phase flows.

Acknowledgements

Authors acknowledge the financial support provided by PETROBRAS. Carlos E. F. do Amaral thanks the support of CAPES through a PNPD post-doctoral grant.

References

Ahmed, W.H. and Ismail, B., 2008, "Innovative Techniques For Two-Phase Flow Measurements", *Recent Patents in Electrical Engineering Journal*, Vol. 1, pp. 1-13.

Gregory, G.A. and Scott, D.S., 1969, "Correlation of liquid slug velocity and frequency in horizontal cocurrent gas-liquid", *AIChE Journal*, Vol. 15, pp. 833-835.

Guevara-López, E., Sanjuan-Galindo, R., Córdova-Aguilar, M.S., Corkidi, G., Ascanio, G. and Galindo, E., 2008, "High-speed visualization of multiphase dispersions in a mixing tank", *Chemical Engineering Research and Design*, Vol. 86, pp. 1382-1387.

Hervieu, E., Jouet, E., and Desbat, L., 2002, "Development and validation of an x-ray tomograph for two-phase flow", Annals of the New York Academy of Sciences, Vol. 972, pp. 87-94.

Da Silva, M.J., Schleicher, E. and Hampel, U., 2007, "Capacitance wire-mesh sensor for fast measurement of phase fraction distributions". *Measurement Science and Technology*, Vol. 18, pp. 2245-2251.

Da Silva, M.J., Thiele, S., Abdulkareem, L., Azzopardi, B.J. and Hampel, U., 2010, "High-resolution gas-oil two-phase flow visualisation with a capacitance wire-mesh sensor", *Flow Measurement and Instrumentation*, Vol. 21, pp. 191-197.

Marple, S.L., 1987, "Digital spectral analysis with applications", Ed. Prentice Hall, Englewood Cliffs, New Jersey, USA.

Mattar, L., Gregory, G.A., 1974, "Air oil slug flow in an upward-inclined pipe – I: Slug velocity, holdup and pressure gradient", *Journal of Canadian Petroleum Technology*, Vol. 13, pp. 69-76.

Prasser, H.-M., Bottger, A., Zschau, J., 1998, "A new electrode mesh tomograph for gas-liquid flows", *Flow Measurement and Instrumentation*, Vol. 9, pp. 111-119.

Prasser, H.-M., Krepper, E. and Lucas, D., 2002, "Evolution of the two-phase flow in a vertical tube – decomposition of gas fraction profiles .according to bubble size classes using wire-mesh sensors", *International Journal of Thermal Sciences*, Vol. 41, pp. 17-28.

Prasser H.-M., Misawa M., and Tiseanu I., 2005, "Comparison between wire-mesh sensor and ultra-fast x-ray tomograph for an air-water flow in a vertical pipe", *Flow Measurement and Instrumentation*, Vol. 16, pp. 73-83.

Szalinski, L., Abdulkareem, L.A., Da Silva, M.J., Thiele, S., Beyer, M., Lucas, D., Hernandez-Perez, V., Hampel, U., Azzopardi, B.J., 2010, "Comparative study of gas-oil and gas-water two-phase flow in a vertical pipe", *Chemical Engineering Science*, Vol. 65, pp. 3836-3848.

Sharaf, S., Da Silva, M.J., Azzopardi B., Hampel, U., Zippe, C., Beyer M., 2010, "Comparison between wire mesh sensor technology and gamma densitometry", Proceedings of the 6th World Congress On Industrial Process Tomography, Bejing, China, pp. 1464-1472.

Wangjiraniran W., Motegi Y., Richter S., Kikura H., Aritomi M., and Yamamoto K., 2003, "Intrusive effect of wire mesh tomography on gas-liquid flow measurement", *Journal of Nuclear Science and Technology*, Vol. 40, pp. 932-940.

Zuber, N., Findlay, J.A., 1965, "Average volumetric concentration in two-phase flow systems", *Journal of Heat Transfer*, Vol. 87, pp 45-468.